



LAWRENCE  
LIVERMORE  
NATIONAL  
LABORATORY

# Metastability And Crystal Structure of The Bialkali Complex Metal Hydride $\text{NaK}(\text{BH}_4)_2$

L. Seballos, J. Z. Zhang, E. Ronnebro, J. L.  
Herberg, E. H. Majzoub

May 28, 2008

Journal of Alloys and Compounds

## **Disclaimer**

---

This document was prepared as an account of work sponsored by an agency of the United States government. Neither the United States government nor Lawrence Livermore National Security, LLC, nor any of their employees makes any warranty, expressed or implied, or assumes any legal liability or responsibility for the accuracy, completeness, or usefulness of any information, apparatus, product, or process disclosed, or represents that its use would not infringe privately owned rights. Reference herein to any specific commercial product, process, or service by trade name, trademark, manufacturer, or otherwise does not necessarily constitute or imply its endorsement, recommendation, or favoring by the United States government or Lawrence Livermore National Security, LLC. The views and opinions of authors expressed herein do not necessarily state or reflect those of the United States government or Lawrence Livermore National Security, LLC, and shall not be used for advertising or product endorsement purposes.

# Metastability And Crystal Structure of The Bialkali Complex Metal Hydride NaK(BH<sub>4</sub>)<sub>2</sub>

Leo Seballos<sup>+</sup>, Jin Z. Zhang<sup>#</sup>, Ewa Ronnebro<sup>±</sup>, Julie L. Herberg<sup>\*</sup>, and E.H. Majzoub<sup>\*</sup>

<sup>+</sup> University of Missouri, Department of Physics and Astronomy and the Center for Nanoscience, St. Louis, MO 63121, USA

<sup>±</sup> Sandia National Laboratories, P.O. Box 969, Livermore, CA 94551, USA

<sup>±</sup> Lawrence Livermore National Laboratories, P.O. Box 808, Livermore, CA 94551, USA

<sup>#</sup> University of California, Department of Chemistry and Biochemistry, Santa Cruz, CA 95064, USA

<sup>\*</sup> Corresponding author

## ABSTRACT

A new bialkali borohydride, NaK(BH<sub>4</sub>)<sub>2</sub>, was synthesized by mechanical milling of NaBH<sub>4</sub> and KBH<sub>4</sub> in a 1:1 ratio. The synthesis was conducted based on a prediction from a computational screening of hydrogen storage materials suggesting the potential stability of NaK(BH<sub>4</sub>)<sub>2</sub>. The new phase was characterized using X-ray diffraction, Raman scattering and magic angle spinning (MAS) nuclear magnetic resonance (NMR). The Raman measurements indicated B-H vibrations of the (BH<sub>4</sub>)<sup>-</sup> anion, while magnetic resonance chemical shifts in <sup>23</sup>Na, and <sup>39</sup>K MAS NMR spectra showed new chemical environments for Na and K resulting from the formation of the new bialkali phase. X-ray diffraction spectra indicated a new crystal structure with rhombohedral symmetry, most likely in the space group R3, distinct from the starting materials NaBH<sub>4</sub>, and KBH<sub>4</sub>. Although *in-situ* XRD measurements indicated the material to be metastable, decomposing to the starting materials NaBH<sub>4</sub> and KBH<sub>4</sub>, the successful synthesis of NaK(BH<sub>4</sub>)<sub>2</sub> demonstrates the ability of computational screening to predict candidates for hydrogen storage materials.

## INTRODUCTION

With the growing concerns over global warming, the development of efficient and clean fuel alternatives has been increasing. Researchers have explored many alternatives to fossil fuels such as methane, biomass, and ethanol, and metal hydrides for hydrogen storage.<sup>1-4</sup> Industry and research institutions have focused efforts to use hydrogen as a fuel for consumer and commercial purposes as an alternative to hydrocarbons given its non-polluting nature and efficiency when used in fuel cells. However, the development of hydrogen storage/delivery systems has yet to meet all of the requirements established by the U.S. Department of Energy for widespread application, and the search for hydrogen storage material candidates continues.<sup>5</sup> Complex metal hydrides have attracted considerable attention due to their high gravimetric hydrogen densities, and several studies have been conducted to improve their performance for applications.<sup>6-10</sup> While

techniques such as mechanical ball milling and doping have improved the hydrogen sorption properties of these materials, few meet all of the desired targets, requiring further search for new complex hydrides.

In this paper, we present the synthesis of a novel bialkali complex metal hydride,  $\text{NaK}(\text{BH}_4)_2$ . The potential stability of this compound was indicated by rapid screening calculations, which predicted that the compound was very weakly unstable against decomposition to the preparation materials,  $\text{NaBH}_4$ , and  $\text{KBH}_4$ , based on first-principles DFT at  $T=0\text{K}$  using a predicted structure generated from a prototype electrostatic ground state (PEGS) search described elsewhere.<sup>11</sup> Attempts to prepare the  $\text{NaK}(\text{BH}_4)_2$  via a ball milling technique was successful and its formation was confirmed using X-ray diffraction, and Raman and solid state nuclear magnetic resonance (NMR) spectroscopy.

## EXPERIMENTAL

All sample preparations were conducted under an inert argon atmosphere with  $\text{O}_2$  and  $\text{H}_2\text{O}$  levels below 1 ppm. The material was synthesized by ball milling 2 grams of  $\text{NaBH}_4$  (Sigma-Aldrich) and  $\text{KBH}_4$  (Sigma-Aldrich) in a 1:1 molar ratio with 4 tungsten carbide balls for 2.5 hours using a SPEX 8000 mechanical mill [denoted sample 1]. A 2 gram sample of 1:1  $\text{NaBH}_4$  and  $\text{KBH}_4$  was also prepared by milling the materials for 30 minutes using a Gilson Company, Inc LC-106 planetary mill rotating at 300 rpm [denoted sample 2]. Analyses of the materials were conducted immediately after milling was complete. X-ray diffraction patterns were obtained using a Rigaku Rotoflex (RU-300ELR) X-ray diffractometer in Debye-Scherrer geometry with the materials in sealed capillary tubes.

Reitveld refinement of the powder X-ray patterns were conducted using the Fullprof program.<sup>12</sup> Refined parameters were: zero point, scale factor, unit cell parameters, UVW, atom positions and isotropic displacement factors. The background was modeled by interpolation between manually chosen points

Raman scattering measurements were obtained in a backscattering geometry using the 532 nm excitation line of a Spectra-Physics Excelsior CW laser at a power of approximately 2 mW. Signal collection was performed using an Acton Spectra Pro 2750 0.750 m spectrograph coupled to a Princeton Instruments (7508-001) CCD spectrometer. All samples were placed in sealed capillaries and 30 second integration scans were obtained for each compound.

Magic Angle Spinning (MAS) NMR measurements were performed on a Bruker Avance 400WB spectrometer with a magnetic field of 9.4 T. Samples were packed in 4-mm MAS rotors and spun at a rate of either 12 kHz (for  $^{23}\text{Na}$ ) or 5 kHz (for  $^{39}\text{K}$ ) in each analysis. The Free Induction Decay (FID) spectra were taken with a single excitation pulse. All spectra were taken at 90 degrees using a pulse width of either 2.1 ms ( $^{23}\text{Na}$ ), or 10 ms ( $^{39}\text{K}$ ).  $\text{NaCl}$  and  $\text{KNO}_3$ , were used as references at 0 ppm for  $^{23}\text{Na}$  and  $^{39}\text{K}$ ,

respectively. All of the samples were sealed in a MAS rotor under nitrogen gas in a glove box. In addition, all of the data was collected in a two hour window after the samples were sealed in the MAS rotor.

## COMPUTATIONAL

Total energy calculations were performed using the Vienna Ab initio Simulation Package (VASP).<sup>13-16</sup> Perdew-Burke-Ernzerhof (PBE) generalized gradient (GGA) pseudopotentials were used with a plane wave energy cutoff of 600 eV.<sup>17</sup> The Brillouin zone for each structure was sampled with a Monkhorst-Pack mesh using a  $k$ -point spacing of less than 0.05 Å<sup>-1</sup>.

Trial structures for NaK(BH<sub>4</sub>)<sub>2</sub> were generated using the prototype electrostatic ground state (PEGS) method described in detail elsewhere.<sup>18</sup> Briefly, crystal structures are generated through a global optimization of the total energy of the crystal. The PEGS Hamiltonian contains electrostatic interactions between ions and a soft sphere repulsive potential to prevent ionic overlap. The tetrahedral BH<sub>4</sub> anions were assumed to be rigid, with a B-H distance of 1.23 Å. Charges on the H, B, Na, and K atoms were -0.25, 0.0, +1.0, and +1.0, respectively. Standard ionic radii of 0.97 Å, and 1.33 Å were used for Na, and K atoms. A hydrogen radius of 1.3 Å was used, based on the H-Na and H-K distances in NaH, KH, and the radii of the cations. Forty-five trial structures were generated using PEGS and subsequently relaxed using first-principles density functional theory to obtain lattice parameters and accurate energetics for decomposition energy estimates. The structures were searched for symmetry using the FINDSYM program in the ISOTROPY software package.<sup>19</sup>

## RESULTS AND DISCUSSION

Crystal structure screening is often approached using a database search where structure types are taken from a large database, such as the Inorganic Crystal Structure Database (ICSD).<sup>20</sup> First-principles calculations of the total energy are performed using structures from the database substituted with the desired chemistry and the lowest being presumed to be a candidate for the ground state. This technique has been successfully applied to the Ca-Al-H system, and had successfully predicted both the CaAlH<sub>5</sub>, and Ca(AlH<sub>4</sub>)<sub>2</sub> structures.<sup>21</sup> When the database has a very limited selection of structure types due to complexity of the compound formula, for example, other methods of structure determination may be necessary. A recently developed structure prediction method using prototype electrostatic ground states (PEGS) has proven to successfully predict many known alanates including NaAlH<sub>4</sub>, Mg(AlH<sub>4</sub>)<sub>2</sub>, and K<sub>2</sub>LiAlH<sub>6</sub>, and has recently produced the best candidate for the ground state structure of Mg(BH<sub>4</sub>)<sub>2</sub>.<sup>21, 22</sup> In addition, the PEGS method produced crystal structure types for compound formula that were not found in the ICSD database. Additions of these structures to the ICSD will allow more successful searches in the future.

PEGS searching produced crystal structures with an upper bound on the cohesive energy of a potential structure. In the case of  $\text{NaK}(\text{BH}_4)_2$ , there may naturally have been a lower energy structure leading to stability against the decomposition reaction  $\text{NaK}(\text{BH}_4)_2 \rightarrow \text{NaBH}_4 + \text{KBH}_4$ . Corrections provided by vibrational contributions to the total free energy also impacts the stability, but were not included in the screening process due to computational expense. The PEGS method, while identifying  $\text{NaK}(\text{BH}_4)_2$  as a potentially stable material, produced several high symmetry crystal structures. Three of the structure types were not found in the ICSD database when using the search string “ABC2X8.” The four highest symmetry crystal structures from the PEGS search for  $\text{NaK}(\text{BH}_4)_2$  were, from lowest to highest symmetry, R3, R-3, P3m1, and R-3m (see Table 1). Remarkably, all generated structures were rhombohedral, belonging to the same fundamental lattice type. The total DFT energies, at  $T=0\text{K}$ , of the four structures were ordered monotonically with the crystal symmetry, with the highest symmetry R-3m having the lowest energy. The P3m1, R-3, and R3 structures had a  $T=0\text{ K}$  total energy of 7.6, 8, and 11 kJ/mol per formula unit above the R-3m structure, respectively. Using the lowest energy R-3m structure for  $\text{NaK}(\text{BH}_4)_2$ , and ignoring the phonon contribution to the total free energy, the decomposition reaction into  $\text{NaBH}_4$  and  $\text{KBH}_4$  was calculated to be approximately -3kJ/mol formula unit at  $T=0\text{ K}$ , indicating that the decomposition would proceed spontaneously. However, zero point energy (ZPE) phonon contributions can be in the range of 5kJ/ mol for low Z compounds. Taken together with the upper bound on the predicted cohesive energy of  $\text{NaK}(\text{BH}_4)_2$ , the potential for stability in  $\text{NaK}(\text{BH}_4)_2$  could not be ruled out.

Figure 1 presents the Raman spectra obtained from  $\text{KBH}_4$ ,  $\text{NaBH}_4$ , sample 1, and sample 2, which shows that peaks assigned to B-H vibrations were clearly seen from all samples.<sup>23, 24</sup> However, the Raman spectrum of sample 2 showed that the B-H bending and stretching modes contained doublet peaks. When the position of these modes were examined in the spectra of the individual  $\text{NaBH}_4$  and  $\text{KBH}_4$  samples, the position of their respective peaks were similar to the composite peaks in the doublets of the spectrum of sample 2.  $\text{KBH}_4$  and  $\text{NaBH}_4$  displayed their respective bending and stretching peaks at  $1255\text{ cm}^{-1}$  and  $1285\text{ cm}^{-1}$ , and  $2315\text{ cm}^{-1}$  and  $2339\text{ cm}^{-1}$  while sample 2 had its doublets at  $1258\text{ cm}^{-1}$  and  $1283\text{ cm}^{-1}$ , and  $2318\text{ cm}^{-1}$  and  $2338\text{ cm}^{-1}$ . This leads us to believe that the Raman signal of sample 2 is a superposition of the Raman signals of the starting materials of  $\text{NaBH}_4$  and  $\text{KBH}_4$ , indicating that the relatively low energy planetary mill technique resulted in a mixture of  $\text{NaBH}_4$  and  $\text{KBH}_4$  instead of forming the desired product. The minor discrepancies in the peak position of sample 2 to those of the individual  $\text{KBH}_4$  and  $\text{NaBH}_4$  materials were likely due to the varying strengths of the signal from the corresponding material. The Raman spectrum of the SPEX-milled material, however, indicated a unique spectral profile observed in sample 1 that could not be obtained by the superposition of the spectra from the starting materials. The new product is presumed to be  $\text{NaK}(\text{BH}_4)_2$ .

The solid state NMR spectra of the samples are shown in Figure 2. The  $^{39}\text{K}$  and  $^{23}\text{Na}$  NMR spectra of the milled sample show peak shifting and broadening due to the

formation of a new compound,  $\text{NaK}(\text{BH}_4)_2$ . In the  $^{39}\text{K}$  NMR, sample **2** and  $\text{KBH}_4$  both presented identical shaped peaks located at 31.38 ppm, while sample **1** had a broader  $^{39}\text{K}$  peak at 32.85 ppm. This shift was likely due to an inequivalent K site resulting from the formation of  $\text{NaK}(\text{BH}_4)_2$ .<sup>25</sup> Similarly, in the  $^{23}\text{Na}$  NMR measurement, sample **2** and  $\text{NaBH}_4$  displayed peaks at -8.25 ppm and -8.15 ppm, respectively. On the other hand, sample **1** had a broadened, shifted peak at -8.52 ppm and a new peak at -14.55 ppm which indicated a new and inequivalent Na site.

XRD spectra were collected within an hour of mechanical milling. In figure 3, the XRD patterns obtained from both sample **2** and sample **1** are presented. The resulting XRD data from sample **2** consisted of peak combinations that belonged only to those of  $\text{NaBH}_4$  and  $\text{KBH}_4$ , with no shifting or broadening visible in the peaks.<sup>26</sup> This was consistent with the Raman measurements. However, an examination of the XRD pattern of sample **1** showed not only the presence of the peaks originating from the starting materials that were broadened and shifted, which indicated that the original material was being transformed, but new peaks were also observed to indicate the new crystal structure attributed to the formation of  $\text{NaK}(\text{BH}_4)_2$ .

In order to determine the stability of this material *in-situ* XRD analyses were conducted immediately after the synthesis. The spectra were collected with varying acquisition times over a 14 hour period, and are presented in Figure 4. Peak areas estimated from the initial XRD spectra (120s scan) indicated an estimated 45% yield of  $\text{NaK}(\text{BH}_4)_2$  was present. However, when longer acquisition scans were conducted to increase the signal to noise ratio, the peaks belonging to  $\text{NaK}(\text{BH}_4)_2$  were reduced in relative intensity, indicating that this hydride was indeed metastable. After approximately 14 hours, the 45 % yield of  $\text{NaK}(\text{BH}_4)_2$  that was initially observed was reduced to approximately 5-10%.

Reitveld refinements, using the theoretically predicted Wyckoff positions and unit cell parameters for the spacegroups  $R\bar{3}$  (no. 146),  $R-3$  (no. 148),  $P3m1$  (no. 156) and  $R-3m$  (no. 166), provided by the PEGS method, were conducted in an attempt to determine the structure of the synthesized  $\text{NaK}(\text{BH}_4)_2$ . Because the compound is metastable and decomposes to  $\text{NaBH}_4$  and  $\text{KBH}_4$ , an X-ray pattern with the highest possible counting statistics was chosen, to some extent sacrificing the highest possible yield of  $\text{NaK}(\text{BH}_4)_2$ . The shifting peak positions as the sample decomposed produced peak profiles that exacerbate the fitting process. For this reason, residuals are presented, but the refined atom coordinates are not reported.

Only Na, K and B atoms in  $\text{NaBH}_4$ ,  $\text{KBH}_4$  and  $\text{NaK}(\text{BH}_4)_2$  were first included in the refinements. The diffraction pattern had amorphous like features, judging from the broad peaks, and possibly also size and strain effects, as evidenced by the large tails of the peaks. Even though the quality of the pattern was not high, an attempt was made to index the new peaks using the trial-and-error program TREOR.<sup>27</sup> The solution with highest figure-of-merit was a hexagonal cell of unit cell with lattice parameters  $a = 4.598\text{\AA}$ , and  $c = 11.209\text{\AA}$ .

First, the structure of  $\text{KBH}_4$  was refined with respect to zero point, scale factor, cell parameters, UVW and displacement factors.<sup>28</sup> The best profile was obtained by using the pseudo-Voigt profile functions and refining against strain. Then,  $\text{NaBH}_4$  was refined and finally the four different structures of  $\text{NaK}(\text{BH}_4)_2$  were tested. For  $\text{NaBH}_4$  and  $\text{NaK}(\text{BH}_4)_2$  ‘Modified 2 Lorentian’ was chosen as profile function. The obtained  $R_B$  values are displayed in Table 2 for three of the trigonal space groups. It was not possible to obtain a good fit for space group  $P3m1$  hence this spacegroup was not considered further.

The difference plot of spacegroup  $R3$ , shown in figure 5, gave the best fit between the observed and calculated patterns, judging from the considerably lower  $R_B$ -value and better fit between observed and calculated diffraction patterns. As indicated in table 2  $R_B$  values for  $R3$ ,  $R-3$  and  $R-3m$  respectively were: 26%, 44% and 40% refined to obtain the same cell parameters. The difference plots (not shown here) of  $R-3$  and  $R-3m$  were very similar, as well as their respective  $R_B$  values. The cell parameters for  $\text{NaK}(\text{BH}_4)_2$  were refined between  $2\theta = 0.3-75^\circ$  in space group  $R3$  ( $Z = 3$ ) to:  $a = 4.615(2)$  and  $c = 22.39(2)$  Å as summarized in Table 3.  $R$ -values of  $R_B = 25.6$  and  $R_F = 21.4\%$  were obtained for the metal atom structure. It was to some extent possible to refine displacement factors and atom coordinates. We note that the refined unit cell has a  $c$ -axis twice as long as the one selected by TREOR, however the smaller unit cell gives unreasonably short atomic bond distances.

By including the predicted H-atom positions in the refinement, the  $R_B$  and  $R_F$  values were lowered to 23.3 and 21.1% respectively, indicating a correct structure model. The  $R$ -values  $R_P = 3.77$ ,  $R_{WP} = 6.64$  indicated a good fit between observed and calculated diffraction patterns. The sample contained 33% of  $\text{NaK}(\text{BH}_4)_2$ , 56% of  $\text{KBH}_4$  and 10% of  $\text{NaBH}_4$ . A total of 49 reflections and 10 soft distance constraints defining an approximately tetrahedral  $\text{BH}_4$  geometry were used for the refinements. The hydrogen atom positions were not refined. It is not expected to obtain better  $R$ -values since the yield of the new material was only 33%. However, it was possible to verify the predicted structure models and to find a preferred atomic arrangement. We conclude that the predicted theoretical structure is most likely the experimental structure of  $\text{NaK}(\text{BH}_4)_2$  based on the data available.

## CONCLUSION

The bialkali borohydride  $\text{NaK}(\text{BH}_4)_2$  was prepared by milling  $\text{NaBH}_4$  and  $\text{KBH}_4$  in a high-energy SPEX mechanical mill. The presence of  $(\text{BH}_4)^-$  anions in the new compound was established with Raman spectroscopy, and the new crystal site environment for Na and K were confirmed with solid state NMR. Rietveld refinement of XRD spectra indicate the spacegroup of  $\text{NaK}(\text{BH}_4)_2$  to be  $R3$ . In-situ X-ray diffraction confirms the predicted metastability of  $\text{NaK}(\text{BH}_4)_2$ , and the material decomposes into the starting compounds after 14 hours.

The successful synthesis of  $\text{NaK}(\text{BH}_4)_2$  demonstrates the potential of the PEGS method and first-principles modeling as a means to select potential materials to explore as hydrogen storage media. By conducting initial stability calculations using this method, the efficiency of pursuing hydrogen storage materials can be increased. Additionally, we have provided three valuable new crystal structure types for addition into the database literature.

## ACKNOWLEDGEMENTS

This project was supported by the Basic Energy Sciences (BES) Division of the US Department of Energy (DOE) and the Office of Energy Efficiency and Renewable Energy (EERE) under the Hydrogen Storage Grand Challenge, Center of Excellence within DOE's National Hydrogen Storage Project. **This work performed under the auspices of the U.S. Department of Energy by Lawrence Livermore National Laboratory under Contract DE-AC52-07NA27344**

## REFERENCE:

1. B. Bogdanovic, M. Schwickardi, J. Alloys Comp. 253-254 (1997) 1.
2. T.V. Choudhary, D.W. Goodman, Catal. Lett. 59 (1999) 93.
3. R.D. Cortright, R.R. Davda, J.A. Dumesic, Nature 418 (2002) 964.
4. G.A. Deluga, J.R. Salge, L.D. Schmidt, X.E. Verykios, Science 303 (YEAR) 993.
5. U. S. Department of Energy Hydrogen Program  
[<http://www.hydrogen.energy.gov>]
6. L. Zaluski, A. Zaluska, J.O. Strom-Olsen, J. Alloys Comp. 290 (1999) 71.
7. E.H. Majzoub, K.J. Gross, J. Alloys Comp. 356 (2003) 363.
8. F. Schuth, B. Bogdanovic, M. Felderhoff, Chem. Commun. 20 (2004) 2249.
9. W. Grochala, P.P. Edwards, Chem. Rev. 104 (2004) 1283.
10. M. Au, A. Jurgensen, J. Phys. Chem. B 110 (2006) 7062.
11. E.H. Majzoub, K.F. McCarty, V. Ozolins, Phys. Rev. B 71 (2005) 024118.
12. J. Rodriguez-Carvajal, PROGRAM FullProf. 2k (Version 3.00- Nov2004-LLB JRC)
13. G. Kresse, J. Hafner, Phys. Rev. B 47 (1993) 558.
14. G. Kresse, J. Hafner, J. Phys. Condes. Matter 6 (1994) 8245.
15. G. Kresse, J. Furthmuller, Comput Mater Sci. 6 (1996) 15.
16. G. Kresse, J. Furthmuller, Phys. Rev. B. 54 111
17. J.P. Perdew, K. Burke, M. Ernzerhof, Phys. Rev. Lett. 77 (1996) 3865.
18. E.H. Majzoub, V. Ozolins, Phys. Rev. B 77 (2008) 104115.
19. ISOTROPY, H.T. Stokes, D.M. Hatch, B.J. Campbell, ISOTROPY (2007)  
[stokes.byu.edu/isotropy.html](http://stokes.byu.edu/isotropy.html).

20. Inorganic Crystal Structure Database, <http://icsd.ill.fr/icsd/index.html>
21. C. Wolverton, V. Ozolins, Phys. Rev. B. 75 (2007) 064101.
22. V. Ozolins, E.H. Majzoub, C. Wolverton, Phys. Rev. Lett. 100 (2008) 135501.
23. K.B. Harvey, N.R. McQuaker, Can. J. Chem. 49 (1971) 3272.
24. G. Renaudin, S. Gomes, H. Hagemann, L. Keller, K. Yvon, J. Alloys Comp. 375 (2004) 98.
25. I.L. Moudrakovski, J.A. Ripmeester, J. Phys. Chem. B 111 ( 2007) 491.
26. Y. Nakamori, K. Miwa, A. Ninomiya, H. Li, N. Ohba, S. Towata, A. Züttel, S. Orimo, Phys. Rev. B 74 (2006) 045126.
27. P.E. Werner, L. Eriksson, M. Westdahl, J. Appl. Crystallogr, 18 (1985) 367.
28. J. Rodriguez-Carvajal, PROGRAM FullProf.2k (Version 3.00 - Nov2004-LLB JRC).

Atom	X	Y	Z
P3m1 a=4.70347 c=7.29140			
H1	2/3	1/3	0.01695
H2	0.38180	0.19090	0.79183
H3	0.04822	0.52411	0.39448
H4	1/3	2/3	0.17121
B1	2/3	1/3	0.84922
B2	1/3	2/3	0.33975
Na1	1/3	2/3	0.68932
K1	0	0	0.15858
R-3 a=4.52898 c=22.22138			
H1	0.62155	0.86403	0.39270
H2	0	0	0.79965
B1	0	0	0.74422
Na1	0	0	0
K1	0	0	1/2
R-3m a=4.59609 c=20.9634			
H1	0	0	0.68029
H2	0.70953	0.85476	0.75869
B1	0	0	0.738605

Na1	0	0	0
K1	0	0	1/2
R3 a=4.55711 c=22.24725			
H1	0.40255	0.08922	0.45477
H2	0	0	0.04844
H3	0.14545	0.85253	0.61091
H4	0	0	0.53710
B1	0	0	0.10374
B2	0	0	0.59207
Na1	0	0	0.85648
K1	0	0	0.35251

Table 2. Comparison of  $R_B$  criteria of fit from the Rietveld refinements of  $\text{NaK}(\text{BH}_4)_2$  in three trigonal space groups, with and without hydrogen atoms included.

<b>Space Group</b>	<b><math>R_B</math> (%) No H</b>	<b><math>R_B</math> (%) With H</b>
<i>R3</i>	26	23
<i>R-3</i>	44	40
<i>R-3m</i>	40	42

Table 3. Summary of unit cell parameters, R-values and phase content as calculated from the Rietveld refinements for the three identified phases. Hydrogen atoms were included in the structure model of NaK(BH<sub>4</sub>)<sub>2</sub>.

Phase	Space Group No.	Unit Cell (Å)	R <sub>B</sub> R <sub>F</sub>	Content (%)
KBH <sub>4</sub>	<i>Fm3m</i> (#225)	<i>a</i> = 6.708(2)	9.26 8.62	53.8
NaBH <sub>4</sub>	<i>Fm3m</i> (#225)	<i>a</i> = 6.208(2)	24.6 19.6	10.7
NaK(BH <sub>4</sub> ) <sub>2</sub>	<i>R3</i> (#146)	<i>a</i> = 4.615(2) <i>c</i> = 22.39(2)	23.3 21.1	35.8

## Figure Captions

Figure 1. Raman spectrum of  $\text{NaBH}_4$ ,  $\text{KBH}_4$ , sample **1** and sample **2**. The signal obtained from sample **2** is a superposition of the signal obtained from the starting material unlike those observed from sample **1**.

Figure 2.  $^{39}\text{K}$  and  $^{23}\text{Na}$  MAS NMR spectra of  $\text{NaBH}_4$ ,  $\text{KBH}_4$ , sample **1** and sample **2**. The arrows indicate the observed peak shifting and broadening in the newly formed material of sample **1**, indicating new chemical environments for both Na and K.

Figure 3. XRD pattern of sample **1** and sample **2**. Sample **2** contains only those peaks assigned to  $\text{NaBH}_4$  and  $\text{KBH}_4$  while the arrows on sample **1** shows new peaks to identifying the presence of a new crystal phase attributed to  $\text{NaK}(\text{BH}_4)_2$ .

Figure 4. In-situ XRD measurements of sample **1**. The arrows show the observed decaying intensity of the peaks associated with  $\text{NaK}(\text{BH}_4)_2$ . The alkali borohydride is metastable and decomposes to the starting materials  $\text{NaBH}_4$  and  $\text{KBH}_4$ .

Figure 5. Difference plot from Rietveld refinements of from top to bottom:  $\text{KBH}_4$ ,  $\text{NaBH}_4$  and  $\text{NaK}(\text{BH}_4)_2$ .

Figures

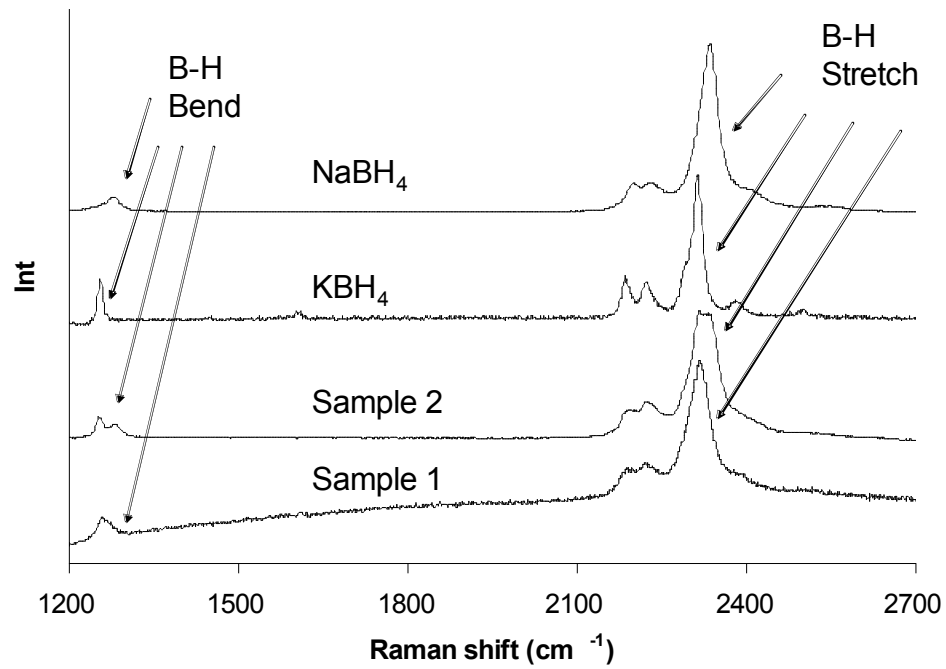


Figure 1

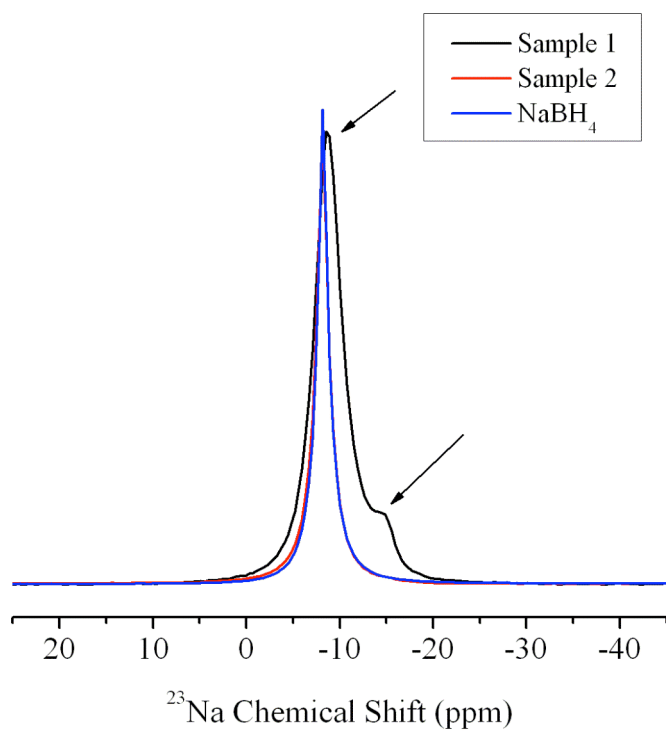
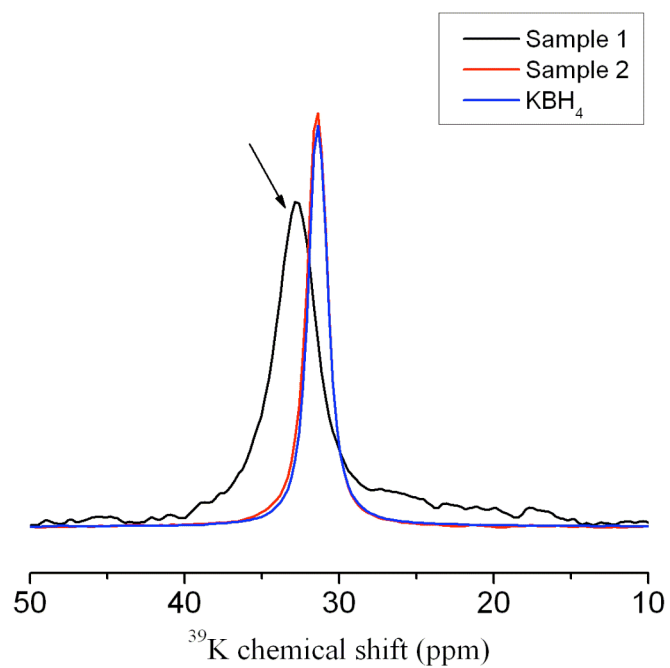


Figure 2

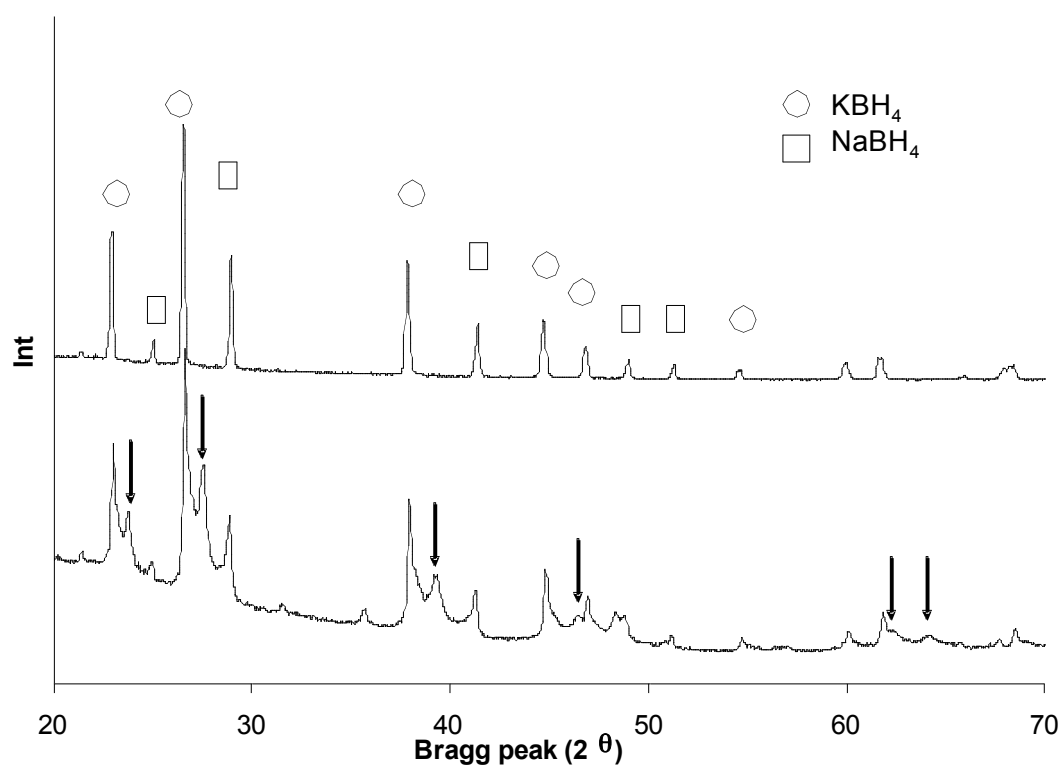


Figure 3

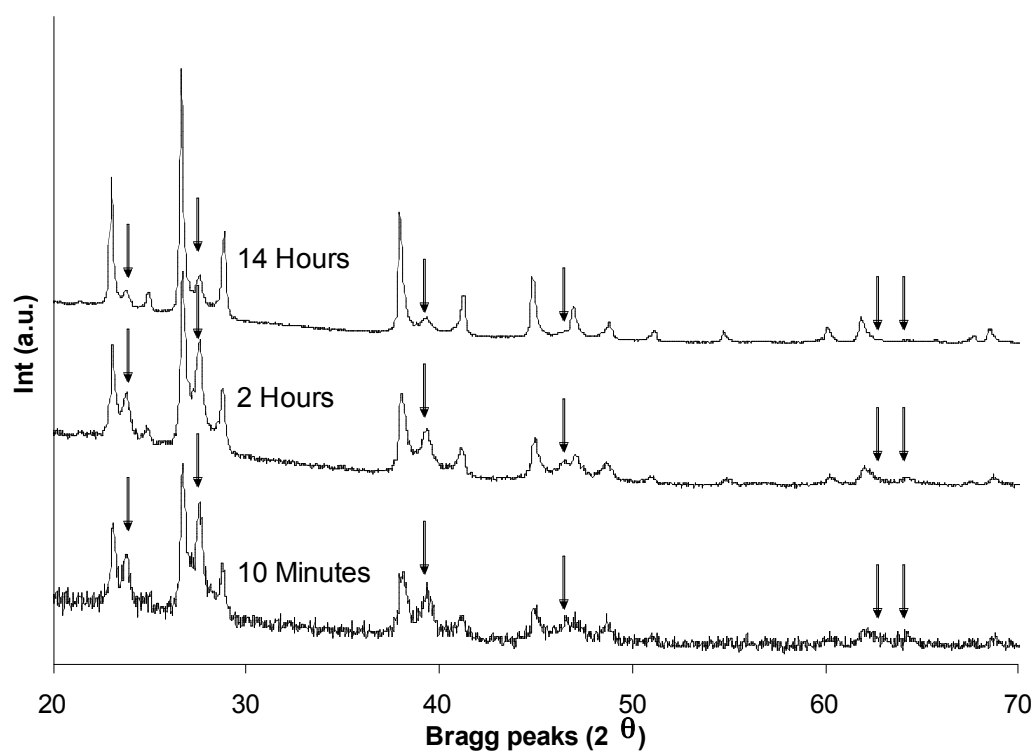


Figure 4

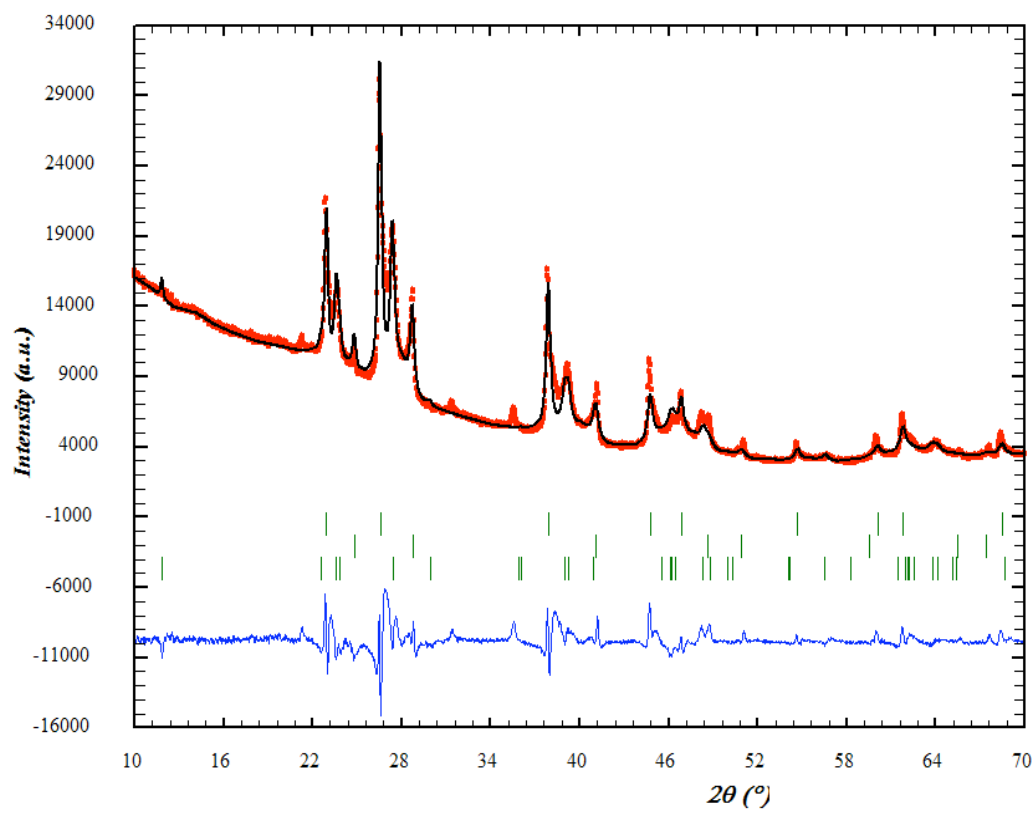


Figure 5